cPLA2 Blockade Attenuates S100A7-Mediated Breast Tumorigenicity by Inhibiting the Immunosuppressive Tumor Microenvironment

SANJAY MISHRA (mishra.174@osu.edu)
The Ohio State University

Manish Charan
The Ohio State University

Rajni Kant Shukla
The Ohio State University

Pranay Agarwal
Stanford University School of Medicine

Swati Misri
The Ohio State University

Ajeet K Verma
The Ohio State University

Dinesh K Ahirwar
The Ohio State University

Jalal Siddiqui
The Ohio State University

Kirti Kaul
The Ohio State University

Neety Sahu
Stanford University School of Medicine

Kunj Vyas
The Ohio State University

Ayush Arpit Garg
The Ohio State University

Anum Khan
The Ohio State University

Wayne O Miles
The Ohio State University

Jonathan W Song
The Ohio State University

Nidhi Bhutani

The Ohio State University

Ramesh K Ganju

The Ohio State University

Research Article

Keywords: Metastasis, breast cancer, S100A7, cPLA2, PGE2, tumor microenvironment

Posted Date: August 26th, 2021

DOI: https://doi.org/10.21203/rs.3.rs-829313/v1

Version of Record: A version of this preprint was published at Journal of Experimental & Clinical Cancer Research on February 8th, 2022. See the published version at https://doi.org/10.1186/s13046-021-02221-0.

Abstract

Background: Metastasis is the major cause of mortality in breast cancer; however, the molecular mechanisms remain elusive. In our previous study, we demonstrated that S100A7/RAGE mediates breast cancer growth and metastasis by recruitment of tumor-associated macrophages. However, the downstream S100A7-mediated inflammatory oncogenic signaling cascade that enhances breast tumor growth and metastasis by generating the immunosuppressive tumor microenvironment (iTME) has not been studied. In this present study, we aimed to investigate the S100A7 and cPLA2 cross-talk in enhancing tumor growth and metastasis through enhancing the iTME.

Methods: Human breast cancer tissue and plasma samples were used to analyze the expression of S100A7, cPLA2, and PGE2 titer. S100A7-overexpressing or downregulated human metastatic breast cancer cells were used to evaluate the S100A7-mediated downstream signaling mechanisms. Bi-transgenic mS100a7a15 overexpression, TNBC C3(1)/Tag transgenic, and humanized patient-derived xenograft mouse models and cPLA2 inhibitor (AACOCF3) were used to investigate the role of S100A7/cPLA2/PGE2 signaling in tumor growth and metastasis. Additionally, CODEX, a highly advanced multiplexed imaging was employed to delineate the effect of S100A7/cPLA2 inhibition on the recruitment of various immune cells.

Results: S100A7 and cPLA2 are highly expressed and positively correlated in malignant breast cancer patients. S100A7/RAGE upregulates cPLA2/PGE2 axis in aggressive breast cancer cells. Furthermore, S100A7 is positively correlated with PGE2 in breast cancer patients. Moreover, cPLA2 pharmacological inhibition suppressed S100A7-mediated tumor growth and metastasis in multiple pre-clinical models. Mechanistically, S100A7-mediated activation of cPLA2 enhances the recruitment of immunosuppressive myeloid cells by increasing PGE2 to fuel breast cancer growth and its secondary spread. We revealed that cPLA2 inhibitor mitigates S100A7-mediated breast tumorigenicity by suppressing the iTME. Furthermore, CODEX imaging data showed that cPLA2 inhibition increased the infiltration of $CD4^+/CD8^+$ T cells in the TME. Analysis of metastatic breast cancer samples revealed a positive correlation between S100A7/cPLA2 with $CD163^+$ tumor-associated M2-macrophages.

Conclusions: Our study shows that cross-talk between S100A7 and cPLA2 plays an important role in enhancing breast tumor growth and metastasis by generating an immunosuppressive tumor microenvironment and reducing infiltration of T cells. Furthermore, S100A7 could be used as a novel non-invasive prognostic marker and cPLA2 inhibitors as promising drugs against S100A7-overexpressing metastatic breast cancer.

Background

Early metastasis to distant organs is a major clinical hurdle in improving the overall and recurrence-free survival of invasive breast cancer patients. Inflammatory immunosuppressive tumor microenvironment (iTME) contributes to cancer cell survival, proliferation, aberrant angiogenesis, early metastasis, and

resistance to established chemo or hormonal therapies [1]. S100A7 (Psoriasin) is a pro-inflammatory secreted protein that regulates breast cancer growth and metastasis [2–4]. Previous reports from others and our group have shown that S100A7 significantly contributes to the breast tumor growth [2–5]. S100A7 mediates breast cancer growth by enhancing inflammatory signaling cascades [5, 6]. S100A7 has been reported to regulate the expression of various pro-inflammatory cytokines such as IL1-α, CXCL-1/8, oncostatin-M, and interleukin-6 [5, 7]. Although S100A7 has been shown to mediate its oncogenic effects through Receptor for Advanced Glycation End-products (RAGE) [8], the downstream inflammatory oncogenic signaling cascades that enhance breast tumor growth and metastasis by modulating the iTME has not been explored. Therefore, understanding the molecular mechanisms that regulate aggressive tumor growth and metastasis may address an unmet medical necessity in invasive breast cancer.

Sustained inflammation is one of the major hallmarks of breast carcinogenesis [9]. Cytosolic phospholipase A2α (cPLA2) plays an important role in the biosynthesis of inflammatory lipids such as Prostaglandin E2 (PGE2) and is shown to drive inflammation-associated cancer progression and metastasis [10–15]. PGE2 also mediates the recruitment of different immunosuppressive cells including macrophages in TME [16]. Macrophages can be classified into two potential subtypes M1 and M2, where M2 exhibits pro-tumor functions [17, 18]. PGE2 was reported to affect the polarization of macrophages in different human malignancies [16, 19]. Inflammatory or anti-inflammatory cytokines/chemokines and growth factors released by M2 macrophages ultimately modulate the iTME. Recently, a chemical inhibitor against cPLA2 has been proven very effective against aberrant angiogenesis in basal-like invasive breast cancer [20]. S100A7 is highly expressed in psoriasis and cPLA2 inhibitors are considered as potent anti-psoriasis agents [21, 22]. Surprisingly, it has been reported that psoriasis predisposes to the development of different cancers [23–25]. However, the crosstalk between S100A7 and cPLA2 in regulating aggressive breast cancer growth and metastasis and its downstream effects in iTME are not known.

In the present study, we performed a systemic in-depth analysis of S100A7 and cPLA2 in breast cancer progression and metastasis using multiple breast cancer cell lines and patient samples. We further exploited different preclinical mice model including mS100a7a15-overexpressing bi-transgenic and humanized patient-derived xenograft (Hu-PDX) mouse models to analyze the pharmacological inhibition of cPLA2 in attenuating S100A7-mediated tumor growth and metastasis. Furthermore, we delineated the cell non-autonomous functions of S100A7/cPLA2 signaling on breast tumorigenesis. Our results reveal that higher co-expression of S100A7 and cPLA2 is associated with worse recurrence free survival in breast cancer patients. In addition, our findings highlight that S100A7/cPLA2 signaling aggravates breast tumor growth and distant metastasis by enhancing the iTME. Altogether, this study identifies S1007/cPLA2 signaling as a promising target against metastatic breast cancers and demonstrate the efficacy of pharmacological inhibition of cPLA2 to improve the clinical outcome of S100A7-overexpressing malignant breast tumors.

Materials And Methods

Cell culture, Reagents and other Analytic methods

Human breast carcinoma cell lines MDA-MB-231 and MDA-MB-468 were obtained from ATCC. MVT-1 cells (derived from MMTV-c-Myc; MMTV-VEGF bi-transgenic mice) were obtained from Dr. Johnson. MVT-1 highly metastatic cells were cultured as described [5, 26]. MDA-MB-231 cell lines were transfected with pIRES2-EGFP-hS100A7 or pIRES-2-EGFP using Lipofectamine-2000 reagent as per manufacturer's instructions and stable S100A7 overexpressing clones were generated using G418 selection (500 mg/mL). Stable S100A7-downregulated MDA-MB-468 cells and PLKO.1-puro vector control cells were cultured as described in our earlier study [2]. BMDM were also isolated from wild type 6-week-old female mice and differentiated into macrophages as described earlier [27]. Dulbecco's modified eagle medium, fetal bovine serum, penicillin and streptomycin antibiotic, trypsin, and ethylene diamine tetra acetic acid were obtained from Gibco BRL (Grand Island, NY, USA). RAGE Antagonist (FPS-ZM1) and recombinant S100A7 were purchased from Calbiochem and Novus Biologicals. Details regarding various analytical methods used in this study including flow cytometry, immunofluorescence (IF), immunohistochemistry (IHC), ELISA, immunoblotting, siRNA transfection, CODEX, patients data analysis and BMDM migration have been provided in **Supplementary material and method section**.

Mouse models

The NSG (NOD scid gamma mouse) mice were obtained from the OSU animal core facility. TetO-mS100a7a15 mice were kindly provided by Dr. Yuspa (NIH). TetO-mS100a7a15 mice [21] were cross-bred with MMTV-rtTA mice to generate bi-transgenic MMTV-mS100a7a15 mice. Transgenic littermates were genotyped by PCR. Female MMTV-mS100a7a15 mice were fed with Dox-chow 1 g/kg (Bio-Serv), and mice with a normal diet served as controls. FVB-Tg(C3-1-TAg)cJeg/JegJ mice (Stock No:013591) were purchased from Jackson laboratory. The metastatic triple-negative breast cancer patient-derived xenograft (TM00096) was purchased from Jackson Lab and the humanized-PDX mouse model was developed as described previously [28, 29]. All mice were kept in The OSU's animal facility in compliance with the guidelines and protocols approved by the OSU-IACUC. MVT-1 cells ($1X10^5$) were injected into the mammary glands of mS100a7a15 overexpression bi-transgenic mice. Transgenic mice injected with MVT-1 cells were fed either with Dox-chow 1g/kg (Tet-on) or a normal diet (Tet-off). Tumors were measured weekly with external calipers and volume was calculated as described earlier and animals were sacrificed and tumors were excised [5].

Statistical Analysis

For continuous variables, two-sample *t*-tests were used if two groups were compared, and One-way ANOVA was used when more than two groups were compared. Non-parametric tests were also used to calculate the p values for comparing the clinical data more than two groups. Spearman's rho correlation analysis was used to calculate the correlation coefficient and p values. * indicates $P < 0.05$; ** indicates $P < 0.01$; *** indicates $P < 0.001$; **** indicates $P < 0.0001$; ns is non-significant.

Results

High co-expression of S100A7 and cPLA2 is correlated with poor clinical prognosis in breast cancer

To investigate the clinical significance of S100A7 and cPLA2 (PLA2G4A) in invasive breast cancer, we first analyzed the protein expression of S100A7 and cPLA2 using human tissue microarray (TMAs) of malignant breast cancer patients by immunohistochemistry analysis. We discovered a significantly higher level of S100A7 and cPLA2 proteins in tumor tissues compared to normal breast tissues (Fig. 1A **& D**). We also observed significantly higher expression of both S100A7 and cPLA2 proteins in high-grade malignant breast tumors compared to the low-grade and normal tissues (**Supplementary Fig. 1A-C**). Next, we evaluated the relative mRNA expression of S100A7 and cPLA2 in low and high-grade breast tumor tissues using different publically available clinical datasets. Using GENT2 database, we observed that higher-grade invasive breast tumors show increased expression of S100A7 and PLA2G4A compared to low-grade tumors (Fig. 1B **& E**). Further, we evaluated whether these results were also found in independent cohorts of breast cancer patients. For this, we analyzed the differential expression of S100A7 and cPLA2 genes across the different stage, grade, and tumor size of breast cancer patients using publically available Caldas and Chin datasets (**Supplementary Fig. 1D)**. In agreement with our previous results, we observed that S100A7 and PLA2G4A revealed significantly higher expression in high-grade tumors compared to low-grade breast tumor tissues (Fig. 1C **& F**). Next, we evaluated the correlation of S100A7 and cPLA2 protein expression using malignant tumor tissue samples of same breast cancer patients. Interestingly, we found a significant positive correlation (Spearman's rho correlation coefficient = 0.544) between S100A7 and cPLA2 protein expression across malignant breast tumor tissue samples (Fig. 1G). We further tested the correlation between S100A7 and PLA2G4A gene expression in breast cancer patients using the SEEK database (Search-Based Exploration of Expression Compendium). We observed a significant positive correlation between S100A7 and PLA2G4A in distinct signal transduction pathways (r = 0.93) and among different breast tumor samples from pre-and post-chemotherapy (r = 0.59) (Fig. 1H). We also evaluated the prognostic significance of S100A7 and PLA2G4A alone or in combination and a recurrence free survival (RFS) probability of breast cancer patients using the Kaplan Meier (KM)-plotter [Breast cancer] tool (gene chip). The KM plotter analysis revealed that alone or combined higher expression of both these two genes had high hazard ratios and significant poor RFS probability among breast cancer subjects (Fig. 1I-K). Interestingly, we sought to analyze the clinical significance of S100A7 and cPLA2 in relapse free survival at 5 years in breast cancer patients treated with any chemotherapy using ROC (receiver operating characteristics) plotter database. ROC plotter database is capable to link gene expression and response to therapy using transcriptome-level data [44]. We discovered that S100A7 and cPLA2 showed significantly decreased expression in responder cohorts as compared to non-responder breast cancer patients with area under curve (AUC) values of 0.571 (205916_at; Mann-Whitney test p-value: 0.0076) and 0.555 (210145_at; Mann-Whitney test p-value: 0.037) respectively **(Supplementary Fig. 1E & F)**. Taken together, these findings show that S100A7 and cPLA2 are highly expressed and positively correlated with high-grade breast tumors, and lower overall survival for breast cancer patients.

cPLA2 inhibition attenuates S100A7-mediated PGE2 production in breast cancer cells

To further interrogate the correlation and determining the role of S100A7 in regulating cPLA2 expression and its downstream signaling, S100A7 overexpressing/downregulated breast cancer cells were analyzed. We observed that S100A7 overexpression enhances cPLA2 expression in MDA-MB-231 cells (Fig. 2A), whereas S100A7 downregulation reduced the cPLA2 expression in MDA-MB-468 cells (Fig. 2B). In our previous study, we have shown that S100A7 mediates its effect by directly binding to the RAGE receptor in breast cancer cells [45]. In this study, we observed that exogenous supplementation of hS100A7 recombinant protein in S100A7 deficient MDA-MB-231 cells that express RAGE caused increased cPLA2 expression **(Supplementary Fig. 1G)**. Therefore, we next tested the effect of RAGE inhibition on cPLA2 levels in S100A7 overexpressing MDA-MB-231 cells. The pharmacological inhibition of RAGE, using the FPS-ZM1 inhibitor, showed a dose-dependent reduction of cPLA2 expression in S100A7 overexpressing MDA-MB-231 cells (Fig. 2C).

Next, we explored the downstream mechanistic pathway regulated by the S100A7/cPLA2 axis in metastatic breast cancer cells. Here, we observed that S100A7 overexpression significantly increases PGE2 level, which was significantly inhibited by cPLA2 inhibitor (AACOCF3) in MDA-MB-231 cells (Fig. 2D). In addition, S100A7 knock down reduced the PGE2 generation that was not further significantly reduced by AACOCF3 in MDA-MB-468 cells (Fig. 2E). We also discovered that cPLA2 knock down in S100A7 expressing breast cancer cells significantly reduced the PGE2 level (Fig. 2F **& G**) **(Supplementary Fig. 1H & I)**. To further determine the clinical significance of S100A7 in regulating the PGE2 titer in breast cancer patients, we analyzed the titer of S100A7 and PGE2 and their correlation in breast cancer patient's blood plasma samples. We discovered that the level of both S100A7/PGE2 were significantly higher in breast cancer patients as compared to normal subjects (Fig. 2H **& I**). We also observed a significant positive correlation (Spearman's rho correlation coefficient = 0.4) between circulating S100A7 and blood PGE2 in breast cancer patients (Fig. 2J). Overall, our data suggest that the cPLA2 inhibition suppressed S100A7-induced PGE2 generation by breast cancer cells.

cPLA2 inhibition abrogates S100A7-mediated tumor burden in orthotopic and spontaneous breast cancer mouse models

To evaluate the preclinical significance of cPLA2 inhibition in S100A7 overexpressing mammary tumors, we assayed the inhibitory effect of AACOCF3 on orthotopic and spontaneous breast cancer mouse models. mS100a7a15 is a paralog of human S100A7, and we have generated a doxycycline (DOX)-inducible bi-transgenic MMTV-mS100a7a15 mouse model [5]. These mice overexpress mS100a7a15 in the mammary glands in presence of DOX. For this study, we injected MVT-1 cells in mammary fat pad of these mice and after the formation of palpable tumors, we divided these mice into 4 different experimental groups: (a) without DOX (normal diet) with vehicle control (Tet-off-VC), (b) without DOX

(normal diet) with AACOCF3 (Tet-off-AF3), (c) DOX diet with vehicle control (Tet-on-VC), and (d) DOX diet with AACOCF3 Tet-on-AF3) (Fig. 3A). Surprisingly, only mice overexpressing mS100a7a15 respond to cPLA2 inhibitor and showed significantly decreased tumor burden after the treatment of AACOCF3 compared to control animals (Fig. 3B-D). Increased expression of mS100a7a15 was confirmed by immunofluorescence assay in MVT-1 tumors under DOX diet (Tet-on) than mice on a normal diet (Tet-off) **(Supplementary Fig. 2A)**. Visceral organ analysis revealed that cPLA2 inhibition significantly reduced lung and liver metastases, preferentially in Tet-on-AF3 group (Fig. 3E**) (Supplementary Fig. 2B**). Importantly, we also observed that cPLA2 inhibition more drastically reduced the size and weight of the spleen from Tet-on (mS100a7a15-high) group compared to Tet-off group (**Supplementary Fig. 2C**). The spleen plays an essential role in neoplastic growth by serving as a reservoir of many biological factors during the different stages of tumor growth [46] and has been reported as an essential extramedullary site that can unceasingly support tumor growth by increasing the infiltration of immunosuppressive myeloid cells into the tumor [47].

We also investigated the inhibitory potential of AACOCF3 on a spontaneous C3(1)/SV40 T/t-antigen transgenic mouse model of human triple-negative breast cancer [48]. We cross-bred MMTV-rtTA;TetO-mS100a7a15 mouse with C3(1)-TAg,C3(1)/Tag (C3-Tag) mouse and animals with C3-Tag;MMTV-rtTA;TetO-mS100a7a15 genotypes were maintained in presence or absence of DOX diet for eight weeks. Mice fed with DOX diet showed significantly higher tumor burden and pulmonary metastasis compared to mice on a normal diet (Fig. 3F-J**)**. Next, we evaluated the anti-tumor effect of AACOCF3 treatment on C3-Tag;MMTV-rtTA;TetO-mS100a7a15 mice fed with DOX diet. We found that AACOCF3 treatment significantly reduced S100A7 enhanced tumor burden and lung metastasis (Fig. 3K-Q**)**. Altogether, our *in-vivo* studies suggest that cPLA2 inhibition tends to be a promising strategy against S100A7 overexpressing metastatic mammary tumors.

S100A7/cPLA2/PGE2 signaling enhances immunosuppressive tumor microenvironment

Breast cancer iTME constituents possess the ability to reprogram tumor growth and distant metastasis; hence, a better understanding of the iTME would help in designing the effective approaches for efficient targeting of S100A7-overexpressing metastatic breast cancers. Hence, we evaluated the functional significance of cPLA2 inhibition in regulating the recruitment of different myeloid cells for generating an iTME. We demonstrated that high expression of the cPLA2 gene positively correlated with the increased abundance of tumor-associated macrophages (TAMs) and myeloid derived suppressor cells (MDSCs) in invasive breast tumor tissues (**Supplementary Fig. 3A-B**).

PGE2 has been reported to play an important role in the generation of an iTME by modulating immunosuppressive myeloid cells (TAMs and MDSCs) in different human malignancies [16]. Here, we investigated the effect of S100A7/cPLA2/PGE2 axis in bone marrow derived macrophages (BMDMs) migration and plasticity by using cPLA2 and EP4 (PGE2 receptor) inhibitors. We observed that S100A7 overexpression significantly increased the migratory potential of BMDMs and treatment of cPLA2

inhibitor (AACOCF3) or EP4 inhibitor (L-161,982) drastically reduced the S100A7/PGE2-induced migration of BMDMs (Fig. 4A **& B) (Supplementary Fig. 3C & D**). To further study whether S100A7/cPLA2/PGE2 axis influences the differentiation of BMDMs into M2-like macrophages ($CD206^{+}MHC\text{-}II^{low}$), BMDMs were treated with EP4 inhibitor or incubated with conditioned media of AACOCF3 treated S100A7 expressing breast cancer cells. We observed a decreased differentiation of BMDMs into $CD206^{+}MHC\text{-}II^{low}$ M2-like macrophages in presence of cPLA2 or EP4 inhibition (Fig. 4C **& D) (Supplementary Fig. 3E**).

Consistent with our *in-vitro* observations, we found that AACOCF3 significantly reduced the blood PGE2 as well as abundance of TAMs and $CD11b^{+}F4/80^{+}$ macrophages in tumor and spleen of only tumor-bearing S100A7-overexpressing mice respectively (Fig. 4E-G**) (Supplementary Fig. 4A-C**). To further analyze the clinical impact of S100A7/cPLA2 signaling in modulating the host immunosuppressive response, we investigated the correlation of these two proteins with the abundance of tumor promoting $CD163^{+}$ M2-TAMs using TMAs of invasive breast cancer patients. Similar to our previous results, we discovered that different grades of malignant breast tumors revealed a significantly increased abundance of $CD163^{+}$ M2-TAMs compared to normal breast tissues (Fig. 4H **& I**) and also revealed a significant positive correlations with increased expression of S100A7 and cPLA2 proteins (Fig. 4J **& K**). Moreover, cPLA2 gene expression is also significantly positively correlated with $CD163^{+}$ M2-TAMs in breast cancer patients (Fig. 4L). Additionally, KM plotter analysis also indicates that high expression of S100A7 with enriched macrophage population significantly associated with poor RFS probability for breast cancer patients, while high S100A7 expression with decreased macrophage showed non-significant clinical outcome (**Supplementary Fig. 4D**).

We also investigated the effect of cPLA2 inhibition on S100A7-mediated recruitment of MDSCs using our mS100a7a15 overexpressing mice. Interestingly, only mS100a7a15-overexpressing bi-transgenic mice bearing MVT1 tumors selectively responded to cPLA2 inhibitor and revealed reduced recruitment of MDSCs both in spleen and breast tumors (Fig. 5A-F). Different subsets of MDSCs promote the development of tumors and metastasis [49]. We observed that the cPLA2 inhibitor selectively reduced the abundance of granulocytic $Ly6G^{+}$ MDSCs only in the spleen of mS100a7a15-overexpressing mice (**Supplementary Fig. 5A-D**). In brief, these results suggest that the S100A7/cPLA2/PGE2 signaling cascade generates an iTME through modulating the recruitment and plasticity of different immunosuppressive myeloid cells, especially TAMs in metastatic breast cancer, and therefore, disrupting this signaling mechanism may heighten the anti-tumor immune response.

cPLA2 inhibition increases the infiltration of T lymphocytes in tumor

The anti-tumor effect of any chemotherapeutic drugs depends on two facets of cancer biology, first, the direct killing of tumor cells, and secondly is their ability to enhance the $CD4^{+}$ and $CD8^{+}$ tumor infiltrating lymphocytes (TILs)-mediated immune response [50, 51]. Therefore, in this study, we utilized CODEX multiplexed imaging technique, which helps us to explore the functional significance of targeting the

S100A7/cPLA2 signaling axis on abundance, cell surface expression, and interactions of different subsets of $CD4^+$ and $CD8^+$ TILs by using our tumor bearing MMTV-mS100a7a15 bi-transgenic mouse model. CODEX is a recently developed highly multiplexed imaging technique that enables the analysis of more than 56 proteins in a single section of tissue through an iterative imaging process [52, 53]. Spatial interaction of host-tumor cells with immune cells and expression levels of different markers can be easily quantified using this multiplexed technique. Using known cell surface markers, this technique has proved to be particularly useful in profiling the precise immune cell populations in healthy and diseased tissues [52, 53]. As we discovered that cPLA2 inhibitor treatment was significantly effective only in the DOX-inducible mouse model of mS100a7a15, therefore in this study, we investigated the anti-tumor effect of AACOCF3 on immune response mediated through $CD4^+$ and $CD8^+$ TILs in mS100a7a15 overexpression group using CODEX.

CODEX was performed using validated antibodies for mouse tumor tissue samples (Fig. 6A) [53]. Since, in our study, CODEX was performed on FFPE breast tumor tissues, we focused our analysis and interpretations on those T cells markers, which showed positive signal in our samples. The in-depth quantitative and cluster analysis revealed that the AACOCF3 treatment increased the infiltration of proliferating ($Ki\text{-}67^+$) and activated (CD11b/CD45R/CD38/CD90.2) $CD4^+$ and $CD8^+$ TILs in breast TME (Fig. 6B **& C; Supplementary Fig. 6**). CD11b, CD38, CD45R, and CD90.2 are murine cell surface markers known to be associated with the activated status of T cells [54–59]. We also analyzed the cell populations expressing CD4, CD8a, CD90.2, CD45R, CD38, CD11b, and Ki-67 using t-SNE plot analysis and we found that AACOCF3 treatment increased the number of CD4, CD8a, CD90.2, CD38, and CD11b positive cells (Fig. 6D). The anti-tumor activity of TILs depends on mutual direct or indirect interaction of different subset of T cells [60–62], therefore we investigated the effect of cPLA2 inhibition on the interaction of proliferating and activated TILs. We presented the cell-cell interaction map in circus and heatmap plots and we observed that AACOCF3 treatment revealed the highest degree of interaction among the different subset of proliferating and activated $CD4^+$ and $CD8^+$ TILs (Fig. 6E **& F**). Finally, we explored the association of $CD4^+$ and $CD8^+$ T cells with cPLA2 (PLA2G4A) gene expression in invasive basal-like breast cancer patients using the TIMER database. Interestingly, we found that cPLA2 differential expression showed a significant negative correlation with $CD4^+$ and $CD8^+$ T cells infiltration (Fig. 6G). In brief, our results showed that the inhibition of S100A7/cPLA2 signaling could increase the infiltration of proliferating and activated $CD4^+$ and $CD8^+$ TILs in breast TME and may mount an enhanced anti-tumor immune response against aggressive metastatic breast cancer cells.

cPLA2 inhibition attenuates tumor progression in humanized PDX mouse model by decreasing tumor-infiltrating immunosuppressive cells

To determine if the S100A7/cPLA2 signaling axis could be exploited as a potential therapeutic target against metastatic breast cancer, we analyzed the clinical utility of cPLA2 inhibitor against breast tumor

growth and metastasis using Hu-PDX mouse model. Hu-PDX breast cancer mouse models are emerging tools for evaluating the efficacy of novel drugs as well as immunotherapies on tumor growth, immune response, metastasis as they recapitulate the histological characteristics of the original tumors. First, we confirmed the expression of both S100A7 and cPLA2 in tumor lysate from PDX specimen (Fig. 7A). According to our previous results, S100A7 modulates the expression of cPLA2 in breast cancer cells, which is why the cPLA2 inhibitor is much more effective in cancer cells that express high levels of S100A7 protein. Therefore, we assessed the anti-tumor activity of AACOCF3 using this Hu-PDX model (Fig. 7B) that replicates the intact human immune system and TME. In agreement with our previous results, we found that AACOCF3 treatment significantly reduced tumor growth and pulmonary metastasis (Fig. 7C-F). We further explored the effect of cPLA2 inhibition on the immunosuppressive immune landscape of breast TME and observed that AACOCF3 treatment significantly reduced the recruitment of total TAMs and M2-TAMs (Fig. 7G **& H**). Interestingly, no significant change in the infiltration of $CD8^+$ T cells while reduced infiltration of $CD4^+$ T cells were detected (**Supplementary Fig. 7A**). Further, we checked the status of $CD4^+$ T cells in the breast TME to predict the status of an adaptive anti-tumor immune response. We observed an increased CTLA-4 expression on $CD4^+$ T cells in the control groups, which limits $CD4^+$ T cell proliferation and its interaction with other immune cells. AACOCF3 treatment significantly reduced CTLA-4^+ $CD4^+$ T cells (Fig. 7I**)** while $PD1^+$ $CD4^+$ T cells were unaffected (**Supplementary Fig. 7B**). cPLA2 regulates the biosynthesis of PGE2 and PGE2 upregulates PD-L1 expression in different cell types [19, 63]. Therefore, we also analyzed the abundance of PD-$L1^+$ tumor cells and found that AACOCF3 significantly decreased the expression of PD-L1 on tumor cells (Fig. 7J). Consequently, our preclinical data using Hu-PDX provide useful information for developing cPLA2 inhibitors against metastatic breast cancers.

Discussion

Distant metastasis is one of the major clinical hurdle for the successful therapies of invasive breast cancer. Given the worst clinical prognosis and lack of established molecular targets in metastatic breast cancer patients, there is an utmost need for a greater understanding of the molecular mechanisms that enhance the metastatic potential of invasive breast cancer cells. This is important for developing better therapies for metastatic breast cancer patients, especially TNBC and basal like-breast cancer patients. S100A7-mediated signaling pathways promote inflammation, which contributes to aggressive breast tumor growth and metastasis [5, 45, 64–66]. Recent clinical data show that the copy number of the chromosomal region containing S100A genes, including S100A7, is amplified in cancer stem cells of TNBC and basal subtypes [67]. However, the S100A7-mediated downstream molecular mechanism which modulate iTME in metastatic breast cancer is not yet explored.

Here, we demonstrate that the S100A7/RAGE axis enhances cPLA2 expression in metastatic breast cancer cells (Fig. 8). Although, S100A7 and cPLA2 individually have been shown to be overexpressed in breast cancer [68, 69], but no study has been performed to show their correlation in metastatic breast cancer. In our present study, Kaplan-Meier (KM) plotter analysis revealed that high co-expression of both

S100A7 and cPLA2 correlates with decreased overall survival of breast cancer patients. In addition, we discovered that S100A7 expression strongly correlated with cPLA2 expression in metastatic breast cancer patients. We also observed that poorly differentiated high-grade breast tumors expressed high level of both S100A7 and cPLA2 as compared to well-differentiated mammary tumors and their adjacent normal tissues. These studies indicate a positive correlation in between S100A7 and cPLA2 in metastatic breast cancer patients and could be used as potential prognostic marker for subsets of breast cancer patients.

We discovered that S100A7 expression regulates the production of PGE2 in breast cancer cells. We further demonstrated that cPLA2 inhibition caused reduced production of PGE2 only in S100A7 expressing breast cancer cells. Interestingly, a positive correlation between S100A7 and PGE2 levels was observed in breast cancer patient samples. Malignant breast tumors contain high levels of PGE2 [70]. This is the first line of evidence, which indicates that S100A7 positively correlated with PGE2 and that could be used as potential circulating biomarkers in metastatic breast cancer.

In various pre-clinical mouse models including the S100A7 overexpression bi-transgenic and Hu-PDX mouse models, we showed that inhibition of S100A7/cPLA2 signaling by using small molecule inhibitor against cPLA2 significantly reduced tumor burden and metastasis. cPLA2 inhibitors have shown improved efficacy in phase I and II clinical trials against psoriasis [22]. Psoriatic skin have been shown to express higher level of Psoriasin (S100A7) and characterized by dense infiltration of macrophages [71, 72]. Our studies also revealed that S100A7 and cPLA2 are positively correlated with the infiltration of $CD163^+$ M2-TAMs in invasive breast tumor tissues. KM plotter analysis also revealed high expression of S100A7 with enriched macrophage populations significantly associated with the poor recurrence-free survival (RFS) of breast cancer patients. In contrast, high S100A7 expression with decreased macrophage density does not predict the patient outcome. Here, we demonstrate that cPLA2 inhibition drastically decreased the infiltration of TAMs in a syngeneic mS100a7a15 overexpressing breast cancer mouse model. In human breast tumors, infiltrating TAMs, which represent up to 50% of the tumor mass, correlates with poor prognostic features, higher tumor grade [73], and decreased disease-free survival [74, 75]. Higher TAM density is typically associated with a higher vascular density, suggesting an angiogenic role of TAMs in human tumors [76]. In this study, we further showed that S100A7/cPLA2 signaling elevated the PGE2 generation that increased migration and polarization of macrophages towards M2-type through the EP4 receptor of BMDM. Interestingly, we also found that inhibition of S100A7/cPLA2 signaling reduced PGE2 level in S100A7 overexpressing pre-clinical breast cancer mouse model. PGE2 has been shown to generate the iTME in different human malignancies by modulating the behavior of different immune cells [16]. Notably, PGE2/EP4 has also been reported to increase the expression of PD-L1 on MDSCs and TAMs [19].

TME is an essential part of solid tumor mass and considered as a promising therapeutic target [77]. The presence of tumor-infiltrating lymphocytes (TILs) in the TME indicates mounting of an immune response against tumor [78]. Recent studies have documented that $CD4^+$ T cells are also effective at tumor rejection similar to $CD8^+$ T cells [79, 80]. Therefore, we utilized a Hu-PDX mouse model to elucidate the effect of cPLA2 inhibition in modulating the tumor-infiltrating $CD4^+$ and $CD8^+$ lymphocytes. We found

that pharmacological inhibition of cPLA2 reduced breast tumor growth and metastasis with a decreased abundance of only CTLA4$^+$ CD4$^+$ T cells and M2-TAMs. In addition, it also decreased the density of PD-L1$^+$ cancer cells to evoke immune evasive mechanisms that prevent CD8$^+$ T cell cytotoxicity [81]. Moreover, CODEX analysis of orthotopic mouse mammary tumors demonstrated that inhibiting S100A7/cPLA2 signaling increased the abundance of proliferating as well as activated CD4$^+$ and CD8$^+$ TILs. Taken together, our study also highlights the potential of cPLA2 inhibitors in increasing the sensitivity of breast cancer cells to existing immunotherapeutic agents.

Conclusion

Our comprehensive studies using *in-vitro* assays, *in-vivo* mouse models, and patient samples showed that a novel cross-talk between S100A7 and cPLA2 enhances breast cancer growth and metastasis. We further showed that S100A7/cPLA2 signaling modulate TME by increasing the recruitment of immunosuppressive myeloid cells and reducing CD4$^+$/CD8$^+$ T cells. Our study provides the usefulness in examining S100A7/cPLA2 expression as potential prognostic marker for invasive and metastatic breast cancer patients. Furthermore, cPLA2 inhibitor could be used a novel therapeutic drug for the treatment of metastatic breast cancer patients who harbor amplification or overexpression of S100A7 gene. Overall, these studies have potential to develop personalized therapy for metastatic breast cancer patients.

Abbreviations

cPLA2: Cytosolic phospholipase A2α, PGE2: Prostaglandin E2, iTME: Immunosuppressive tumor microenvironment, TNBC: Triple negative breast cancer, CODEX, CO-Detection by indEXing, RAGE, Receptor for Advanced Glycation End-products, NSG: NOD scid gamma mouse, MMTV: Mouse mammary tumor virus, VEGF: Vascular endothelial growth factor, TIL: Tumor infiltrating lymphocytes, PD1: Programmed cell death protein 1, PDL1: Programmed death-ligand 1, CTLA4: Cytotoxic T-Lymphocyte Associated Protein 4, TAM: Tumor associated macrophages, MDSC: Myeloid derived suppressor cell, BMDM: bone marrow derived macrophages, KM: Kaplan Meier, ROC: Receiver operating characteristics, AUC: Area under curve, SEEK: Search-Based Exploration of Expression Compendium, TMA: Tissue microarray, HuPDX: Humanized patient derived xenograft, IHC: Immunohistochemistry, IF: Immunofluorescence, ELISA: Enzyme-linked immunosorbent assay. OSU: Ohio State University.

Declarations

Ethical Approval and Consent to participate

All animal experiments were carried out in The Ohio State University's (OSU) animal facility in compliance with the guidelines and protocols approved by the OSU-IACUC. Patient samples were collected on a tissue/blood-collection protocol approved by the OSU IRB. cPLA2

Consent for publication

Not applicable.

Availability of supporting data

All data generated during this study are included in this published article and its supplementary files.

Competing interests

RKG serves as consultant for Guidepoint consultation. Other authors declare no conflict of interest.

Funding

This work was supported by grants from NIH (CA109527 and CA153490) and Department of Defense Breast Cancer Breakthrough Award (W81XWH1910088) and OSU-Comprehensive Cancer Center (CCC) Pelotonia Idea award to RKG. SM, DKA, and KK were supported by Pelotonia Fellowship from the, OSU CCC.

Authors' contributions

Conception, design, interpretation, and manuscript writing and revision: SM, MC, RKG

Data acquisition, statistical and computational analysis, and technical support: SM, MC, RKS, PA, SM, AV, DKA, JS, KK, NS, KV, AAG, AK, WOM, JWS, NB, RKG.

Study supervision: RKG

Acknowledgements

We thank Christina Hopkins for assistance with immunohistochemistry. We also like to thank Charles River for providing a humanized mice model for our PDX study. We would like to acknowledge Dr. Reena Shakya and Target Validation Shared Resource (TVSR) for generating PDX and hu-PDX mice model. We also like to acknowledge OSUCCC for providing confocal and flow cytometry facilities.

Authors' information

[1]Department of Pathology, College of Medicine, The Ohio State University, Columbus, Ohio, USA, 43210. [2]Comprehensive Cancer Center, The Ohio State University, Columbus, OH, USA, 43210. [3] Department of Microbial, Infection & Immunity, The Ohio State University, Columbus, OH, USA, 43210. [4]Department of Cancer Biology and Genetics, The Ohio State University, Columbus, OH 43210, USA. [5]Department of Mechanical and Aerospace Engineering, The Ohio State University, Columbus, OH, USA, 43210. [6]Department of Orthopaedic Surgery, Stanford University, Stanford, CA 94305, USA. [7]School of Medicine, Cell Science Imaging Facility, Stanford University, Stanford, CA 94305, USA.

References

1. Wu Y, Zhou BP: **Inflammation: a driving force speeds cancer metastasis**. *Cell Cycle* 2009, **8**(20):3267-3273.
2. Paruchuri V, Prasad A, McHugh K, Bhat HK, Polyak K, Ganju RK: **S100A7-downregulation inhibits epidermal growth factor-induced signaling in breast cancer cells and blocks osteoclast formation**. *PLoS One* 2008, **3**(3):e1741.
3. Liu H, Wang L, Wang X, Cao Z, Yang Q, Zhang K: **S100A7 enhances invasion of human breast cancer MDA-MB-468 cells through activation of nuclear factor-kappaB signaling**. *World J Surg Oncol* 2013, **11**:93.
4. Krop I, Marz A, Carlsson H, Li X, Bloushtain-Qimron N, Hu M, Gelman R, Sabel MS, Schnitt S, Ramaswamy S *et al*: **A putative role for psoriasin in breast tumor progression**. *Cancer Res* 2005, **65**(24):11326-11334.
5. Nasser MW, Qamri Z, Deol YS, Ravi J, Powell CA, Trikha P, Schwendener RA, Bai XF, Shilo K, Zou X *et al*: **S100A7 enhances mammary tumorigenesis through upregulation of inflammatory pathways**. *Cancer Res* 2012, **72**(3):604-615.
6. Wilkie T, Verma AK, Zhao H, Charan M, Ahirwar DK, Kant S, Pancholi V, Mishra S, Ganju RK: **Lipopolysaccharide from the commensal microbiota of the breast enhances cancer growth: role of S100A7 and TLR4**. *Mol Oncol* 2021.
7. West NR, Watson PH: **S100A7 (psoriasin) is induced by the proinflammatory cytokines oncostatin-M and interleukin-6 in human breast cancer**. *Oncogene* 2010, **29**(14):2083-2092.
8. Wolf R, Howard OM, Dong HF, Voscopoulos C, Boeshans K, Winston J, Divi R, Gunsior M, Goldsmith P, Ahvazi B *et al*: **Chemotactic activity of S100A7 (Psoriasin) is mediated by the receptor for advanced glycation end products and potentiates inflammation with highly homologous but functionally distinct S100A15**. *J Immunol* 2008, **181**(2):1499-1506.
9. Suman S, Sharma PK, Rai G, Mishra S, Arora D, Gupta P, Shukla Y: **Current perspectives of molecular pathways involved in chronic inflammation-mediated breast cancer**. *Biochem Biophys Res Commun* 2016, **472**(3):401-409.
10. Abbott MJ, Tang T, Sul HS: **The Role of Phospholipase A(2)-derived Mediators in Obesity**. *Drug Discov Today Dis Mech* 2010, **7**(3-4):e213-e218.
11. Bhardwaj P, Du B, Zhou XK, Sue E, Giri D, Harbus MD, Falcone DJ, Hudis CA, Subbaramaiah K, Dannenberg AJ: **Estrogen Protects against Obesity-Induced Mammary Gland Inflammation in Mice**. *Cancer Prev Res (Phila)* 2015, **8**(8):751-759.
12. Greenhough A, Smartt HJ, Moore AE, Roberts HR, Williams AC, Paraskeva C, Kaidi A: **The COX-2/PGE2 pathway: key roles in the hallmarks of cancer and adaptation to the tumour microenvironment**. *Carcinogenesis* 2009, **30**(3):377-386.
13. Wang D, Fu L, Sun H, Guo L, DuBois RN: **Prostaglandin E2 Promotes Colorectal Cancer Stem Cell Expansion and Metastasis in Mice**. *Gastroenterology* 2015, **149**(7):1884-1895 e1884.
14. Loo TM, Kamachi F, Watanabe Y, Yoshimoto S, Kanda H, Arai Y, Nakajima-Takagi Y, Iwama A, Koga T, Sugimoto Y *et al*: **Gut Microbiota Promotes Obesity-Associated Liver Cancer through PGE2-Mediated**

Suppression of Antitumor Immunity. *Cancer Discov* 2017, **7**(5):522-538.

15. Linkous A, Geng L, Lyshchik A, Hallahan DE, Yazlovitskaya EM: **Cytosolic phospholipase A2: targeting cancer through the tumor vasculature**. *Clin Cancer Res* 2009, **15**(5):1635-1644.
16. Wang D, DuBois RN: **The Role of Prostaglandin E(2) in Tumor-Associated Immunosuppression**. *Trends Mol Med* 2016, **22**(1):1-3.
17. Pollard JW: **Tumour-educated macrophages promote tumour progression and metastasis**. *Nat Rev Cancer* 2004, **4**(1):71-78.
18. Sica A, Mantovani A: **Macrophage plasticity and polarization: in vivo veritas**. *J Clin Invest* 2012, **122**(3):787-795.
19. Prima V, Kaliberova LN, Kaliberov S, Curiel DT, Kusmartsev S: **COX2/mPGES1/PGE2 pathway regulates PD-L1 expression in tumor-associated macrophages and myeloid-derived suppressor cells**. *Proc Natl Acad Sci U S A* 2017, **114**(5):1117-1122.
20. Kim E, Tunset HM, Cebulla J, Vettukattil R, Helgesen H, Feuerherm AJ, Engebraten O, Maelandsmo GM, Johansen B, Moestue SA: **Anti-vascular effects of the cytosolic phospholipase A2 inhibitor AVX235 in a patient-derived basal-like breast cancer model**. *BMC Cancer* 2016, **16**:191.
21. Wolf R, Mascia F, Dharamsi A, Howard OM, Cataisson C, Bliskovski V, Winston J, Feigenbaum L, Lichti U, Ruzicka T *et al*: **Gene from a psoriasis susceptibility locus primes the skin for inflammation**. *Sci Transl Med* 2010, **2**(61):61ra90.
22. Kokotou MG, Limnios D, Nikolaou A, Psarra A, Kokotos G: **Inhibitors of phospholipase A2 and their therapeutic potential: an update on patents (2012-2016)**. *Expert Opin Ther Pat* 2017, **27**(2):217-225.
23. Vaengebjerg S, Skov L, Egeberg A, Loft ND: **Prevalence, Incidence, and Risk of Cancer in Patients With Psoriasis and Psoriatic Arthritis: A Systematic Review and Meta-analysis**. *JAMA Dermatol* 2020, **156**(4):421-429.
24. Trafford AM, Parisi R, Kontopantelis E, Griffiths CEM, Ashcroft DM: **Association of Psoriasis With the Risk of Developing or Dying of Cancer: A Systematic Review and Meta-analysis**. *JAMA Dermatol* 2019, **155**(12):1390-1403.
25. Fu Y, Lee CH, Chi CC: **Association of Psoriasis with Colorectal Cancer: A Systematic Review and Meta-Analysis**. *J Am Acad Dermatol* 2020.
26. Wolford CC, McConoughey SJ, Jalgaonkar SP, Leon M, Merchant AS, Dominick JL, Yin X, Chang Y, Zmuda EJ, O'Toole SA *et al*: **Transcription factor ATF3 links host adaptive response to breast cancer metastasis**. *J Clin Invest* 2013, **123**(7):2893-2906.
27. Gersuk GM, Razai LW, Marr KA: **Methods of in vitro macrophage maturation confer variable inflammatory responses in association with altered expression of cell surface dectin-1**. *J Immunol Methods* 2008, **329**(1-2):157-166.
28. Zhao Y, Shuen TWH, Toh TB, Chan XY, Liu M, Tan SY, Fan Y, Yang H, Lyer SG, Bonney GK *et al*: **Development of a new patient-derived xenograft humanised mouse model to study human-specific tumour microenvironment and immunotherapy**. *Gut* 2018, **67**(10):1845-1854.

29. Wang M, Yao LC, Cheng M, Cai D, Martinek J, Pan CX, Shi W, Ma AH, De Vere White RW, Airhart S *et al*: **Humanized mice in studying efficacy and mechanisms of PD-1-targeted cancer immunotherapy**. *FASEB J* 2018, **32**(3):1537-1549.
30. Hosein AN, Huang H, Wang Z, Parmar K, Du W, Huang J, Maitra A, Olson E, Verma U, Brekken RA: **Cellular heterogeneity during mouse pancreatic ductal adenocarcinoma progression at single-cell resolution**. *JCI Insight* 2019, **5**.
31. Charan M, Das S, Mishra S, Chatterjee N, Varikuti S, Kaul K, Misri S, Ahirwar DK, Satoskar AR, Ganju RK: **Macrophage migration inhibitory factor inhibition as a novel therapeutic approach against triple-negative breast cancer**. *Cell Death Dis* 2020, **11**(9):774.
32. Suman S, Basak T, Gupta P, Mishra S, Kumar V, Sengupta S, Shukla Y: **Quantitative proteomics revealed novel proteins associated with molecular subtypes of breast cancer**. *J Proteomics* 2016, **148**:183-193.
33. Gupta P, Suman S, Mishra M, Mishra S, Srivastava N, Kumar V, Singh PK, Shukla Y: **Autoantibodies against TYMS and PDLIM1 proteins detected as circulatory signatures in Indian breast cancer patients**. *Proteomics Clin Appl* 2016, **10**(5):564-573.
34. Deol YS, Nasser MW, Yu L, Zou X, Ganju RK: **Tumor-suppressive effects of psoriasin (S100A7) are mediated through the beta-catenin/T cell factor 4 protein pathway in estrogen receptor-positive breast cancer cells**. *J Biol Chem* 2011, **286**(52):44845-44854.
35. Cam M, Charan M, Welker AM, Dravid P, Studebaker AW, Leonard JR, Pierson CR, Nakano I, Beattie CE, Hwang EI *et al*: **DeltaNp73/ETS2 complex drives glioblastoma pathogenesis- targeting downstream mediators by rebastinib prolongs survival in preclinical models of glioblastoma**. *Neuro Oncol* 2020, **22**(3):345-356.
36. Charan M, Dravid P, Cam M, Audino A, Gross AC, Arnold MA, Roberts RD, Cripe TP, Pertsemlidis A, Houghton PJ *et al*: **GD2-directed CAR-T cells in combination with HGF-targeted neutralizing antibody (AMG102) prevent primary tumor growth and metastasis in Ewing sarcoma**. *Int J Cancer* 2020, **146**(11):3184-3195.
37. Mishra S, Srivastava AK, Suman S, Kumar V, Shukla Y: **Circulating miRNAs revealed as surrogate molecular signatures for the early detection of breast cancer**. *Cancer Lett* 2015, **369**(1):67-75.
38. Naderi A, Teschendorff AE, Barbosa-Morais NL, Pinder SE, Green AR, Powe DG, Robertson JF, Aparicio S, Ellis IO, Brenton JD *et al*: **A gene-expression signature to predict survival in breast cancer across independent data sets**. *Oncogene* 2007, **26**(10):1507-1516.
39. Chin K, DeVries S, Fridlyand J, Spellman PT, Roydasgupta R, Kuo WL, Lapuk A, Neve RM, Qian Z, Ryder T *et al*: **Genomic and transcriptional aberrations linked to breast cancer pathophysiologies**. *Cancer Cell* 2006, **10**(6):529-541.
40. Goldman MJ, Craft B, Hastie M, Repecka K, McDade F, Kamath A, Banerjee A, Luo Y, Rogers D, Brooks AN *et al*: **Visualizing and interpreting cancer genomics data via the Xena platform**. *Nat Biotechnol* 2020, **38**(6):675-678.

41. Nagy A, Lanczky A, Menyhart O, Gyorffy B: **Validation of miRNA prognostic power in hepatocellular carcinoma using expression data of independent datasets**. *Sci Rep* 2018, **8**(1):9227.
42. Zhang X, Goncalves R, Mosser DM: **The isolation and characterization of murine macrophages**. *Curr Protoc Immunol* 2008, **Chapter 14**:Unit 14 11.
43. Rentz T, Wanschel A, de Carvalho Moi L, Lorza-Gil E, de Souza JC, Dos Santos RR, Oliveira HCF: **The Anti-atherogenic Role of Exercise Is Associated With the Attenuation of Bone Marrow-Derived Macrophage Activation and Migration in Hypercholesterolemic Mice**. *Front Physiol* 2020, **11**:599379.
44. Fekete JT, Gyorffy B: **ROCplot.org: Validating predictive biomarkers of chemotherapy/hormonal therapy/anti-HER2 therapy using transcriptomic data of 3,104 breast cancer patients**. *Int J Cancer* 2019, **145**(11):3140-3151.
45. Nasser MW, Wani NA, Ahirwar DK, Powell CA, Ravi J, Elbaz M, Zhao H, Padilla L, Zhang X, Shilo K *et al*: **RAGE mediates S100A7-induced breast cancer growth and metastasis by modulating the tumor microenvironment**. *Cancer Res* 2015, **75**(6):974-985.
46. Yamagishi H, Oka T, Hashimoto I, Pellis NR, Kahan BD: **The role of the spleen in tumor bearing host: I. Characterization of spleen cells in tumor-bearing mice**. *Jpn J Surg* 1984, **14**(1):61-71.
47. Cortez-Retamozo V, Etzrodt M, Newton A, Rauch PJ, Chudnovskiy A, Berger C, Ryan RJ, Iwamoto Y, Marinelli B, Gorbatov R *et al*: **Origins of tumor-associated macrophages and neutrophils**. *Proc Natl Acad Sci U S A* 2012, **109**(7):2491-2496.
48. Hoenerhoff MJ, Shibata MA, Bode A, Green JE: **Pathologic progression of mammary carcinomas in a C3(1)/SV40 T/t-antigen transgenic rat model of human triple-negative and Her2-positive breast cancer**. *Transgenic Res* 2011, **20**(2):247-259.
49. Youn JI, Nagaraj S, Collazo M, Gabrilovich DI: **Subsets of myeloid-derived suppressor cells in tumor-bearing mice**. *J Immunol* 2008, **181**(8):5791-5802.
50. Bracci L, Schiavoni G, Sistigu A, Belardelli F: **Immune-based mechanisms of cytotoxic chemotherapy: implications for the design of novel and rationale-based combined treatments against cancer**. *Cell Death Differ* 2014, **21**(1):15-25.
51. Zitvogel L, Apetoh L, Ghiringhelli F, Kroemer G: **Immunological aspects of cancer chemotherapy**. *Nat Rev Immunol* 2008, **8**(1):59-73.
52. Goltsev Y, Samusik N, Kennedy-Darling J, Bhate S, Hale M, Vazquez G, Black S, Nolan GP: **Deep Profiling of Mouse Splenic Architecture with CODEX Multiplexed Imaging**. *Cell* 2018, **174**(4):968-981 e915.
53. Schurch CM, Bhate SS, Barlow GL, Phillips DJ, Noti L, Zlobec I, Chu P, Black S, Demeter J, McIlwain DR *et al*: **Coordinated Cellular Neighborhoods Orchestrate Antitumoral Immunity at the Colorectal Cancer Invasive Front**. *Cell* 2020, **182**(5):1341-1359 e1319.
54. Haeryfar SM, Hoskin DW: **Thy-1: more than a mouse pan-T cell marker**. *J Immunol* 2004, **173**(6):3581-3588.
55. Sandoval-Montes C, Santos-Argumedo L: **CD38 is expressed selectively during the activation of a subset of mature T cells with reduced proliferation but improved potential to produce cytokines**. *J*

Leukoc Biol 2005, **77**(4):513-521.

56. Wang YY, Zhou N, Liu HS, Gong XL, Zhu R, Li XY, Sun Z, Zong XH, Li NN, Meng CT *et al*: **Circulating activated lymphocyte subsets as potential blood biomarkers of cancer progression**. *Cancer Med* 2020, **9**(14):5086-5094.
57. Watanabe Y, Akaike T: **Activation signal induces the expression of B cell-specific CD45R epitope (6B2) on murine T cells**. *Scand J Immunol* 1994, **39**(5):419-425.
58. Luqman M, Bottomly K: **Activation requirements for CD4+ T cells differing in CD45R expression**. *J Immunol* 1992, **149**(7):2300-2306.
59. McFarland HI, Nahill SR, Maciaszek JW, Welsh RM: **CD11b (Mac-1): a marker for CD8+ cytotoxic T cell activation and memory in virus infection**. *J Immunol* 1992, **149**(4):1326-1333.
60. Ostroumov D, Fekete-Drimusz N, Saborowski M, Kuhnel F, Woller N: **CD4 and CD8 T lymphocyte interplay in controlling tumor growth**. *Cell Mol Life Sci* 2018, **75**(4):689-713.
61. Cardenas MA, Prokhnevska N, Kissick HT: **Organized immune cell interactions within tumors sustain a productive T-cell response**. *Int Immunol* 2021, **33**(1):27-37.
62. Ahmed KA, Wang L, Xiang J: **A new dynamic model of three cell interactions for CTL responses**. *Oncoimmunology* 2012, **1**(8):1430-1432.
63. Koundouros N, Karali E, Tripp A, Valle A, Inglese P, Perry NJS, Magee DJ, Anjomani Virmouni S, Elder GA, Tyson AL *et al*: **Metabolic Fingerprinting Links Oncogenic PIK3CA with Enhanced Arachidonic Acid-Derived Eicosanoids**. *Cell* 2020, **181**(7):1596-1611 e1527.
64. Zhao H, Wilkie T, Deol Y, Sneh A, Ganju A, Basree M, Nasser MW, Ganju RK: **miR-29b defines the pro-/anti-proliferative effects of S100A7 in breast cancer**. *Mol Cancer* 2015, **14**(1):11.
65. Batycka-Baran A, Hattinger E, Zwicker S, Summer B, Zack Howard OM, Thomas P, Szepietowski JC, Ruzicka T, Prinz JC, Wolf R: **Leukocyte-derived koebnerisin (S100A15) and psoriasin (S100A7) are systemic mediators of inflammation in psoriasis**. *J Dermatol Sci* 2015, **79**(3):214-221.
66. Leon R, Murray JI, Cragg G, Farnell B, West NR, Pace TC, Watson PH, Bohne C, Boulanger MJ, Hof F: **Identification and characterization of binding sites on S100A7, a participant in cancer and inflammation pathways**. *Biochemistry* 2009, **48**(44):10591-10600.
67. Goh JY, Feng M, Wang W, Oguz G, Yatim S, Lee PL, Bao Y, Lim TH, Wang P, Tam WL *et al*: **Chromosome 1q21.3 amplification is a trackable biomarker and actionable target for breast cancer recurrence**. *Nat Med* 2017, **23**(11):1319-1330.
68. Al-Haddad S, Zhang Z, Leygue E, Snell L, Huang A, Niu Y, Hiller-Hitchcock T, Hole K, Murphy LC, Watson PH: **Psoriasin (S100A7) expression and invasive breast cancer**. *Am J Pathol* 1999, **155**(6):2057-2066.
69. Chen L, Fu H, Luo Y, Chen L, Cheng R, Zhang N, Guo H: **cPLA2alpha mediates TGF-beta-induced epithelial-mesenchymal transition in breast cancer through PI3k/Akt signaling**. *Cell Death Dis* 2017, **8**(4):e2728.

70. Schrey MP, Patel KV: **Prostaglandin E2 production and metabolism in human breast cancer cells and breast fibroblasts. Regulation by inflammatory mediators**. *Br J Cancer* 1995, **72**(6):1412-1419.
71. Madsen P, Rasmussen HH, Leffers H, Honore B, Dejgaard K, Olsen E, Kiil J, Walbum E, Andersen AH, Basse B *et al*: **Molecular cloning, occurrence, and expression of a novel partially secreted protein "psoriasin" that is highly up-regulated in psoriatic skin**. *J Invest Dermatol* 1991, **97**(4):701-712.
72. Clark RA, Kupper TS: **Misbehaving macrophages in the pathogenesis of psoriasis**. *J Clin Invest* 2006, **116**(8):2084-2087.
73. Lee AH, Happerfield LC, Bobrow LG, Millis RR: **Angiogenesis and inflammation in invasive carcinoma of the breast**. *J Clin Pathol* 1997, **50**(8):669-673.
74. Campbell MJ, Tonlaar NY, Garwood ER, Huo D, Moore DH, Khramtsov AI, Au A, Baehner F, Chen Y, Malaka DO *et al*: **Proliferating macrophages associated with high grade, hormone receptor negative breast cancer and poor clinical outcome**. *Breast Cancer Res Treat*, **128**(3):703-711.
75. Leek RD, Lewis CE, Whitehouse R, Greenall M, Clarke J, Harris AL: **Association of macrophage infiltration with angiogenesis and prognosis in invasive breast carcinoma**. *Cancer Res* 1996, **56**(20):4625-4629.
76. Morita Y, Zhang R, Leslie M, Adhikari S, Hasan N, Chervoneva I, Rui H, Tanaka T: **Pathologic evaluation of tumor-associated macrophage density and vessel inflammation in invasive breast carcinomas**. *Oncol Lett* 2017, **14**(2):2111-2118.
77. Zhong S, Jeong JH, Chen Z, Chen Z, Luo JL: **Targeting Tumor Microenvironment by Small-Molecule Inhibitors**. *Transl Oncol* 2020, **13**(1):57-69.
78. Disis ML, Stanton SE: **Triple-negative breast cancer: immune modulation as the new treatment paradigm**. *Am Soc Clin Oncol Educ Book* 2015:e25-30.
79. Perez-Diez A, Joncker NT, Choi K, Chan WF, Anderson CC, Lantz O, Matzinger P: **CD4 cells can be more efficient at tumor rejection than CD8 cells**. *Blood* 2007, **109**(12):5346-5354.
80. Egelston CA, Avalos C, Tu TY, Rosario A, Wang R, Solomon S, Srinivasan G, Nelson MS, Huang Y, Lim MH *et al*: **Resident memory CD8+ T cells within cancer islands mediate survival in breast cancer patients**. *JCI Insight* 2019, **4**(19).
81. Juneja VR, McGuire KA, Manguso RT, LaFleur MW, Collins N, Haining WN, Freeman GJ, Sharpe AH: **PD-L1 on tumor cells is sufficient for immune evasion in immunogenic tumors and inhibits CD8 T cell cytotoxicity**. *J Exp Med* 2017, **214**(4):895-904.

Figures

Figure 1

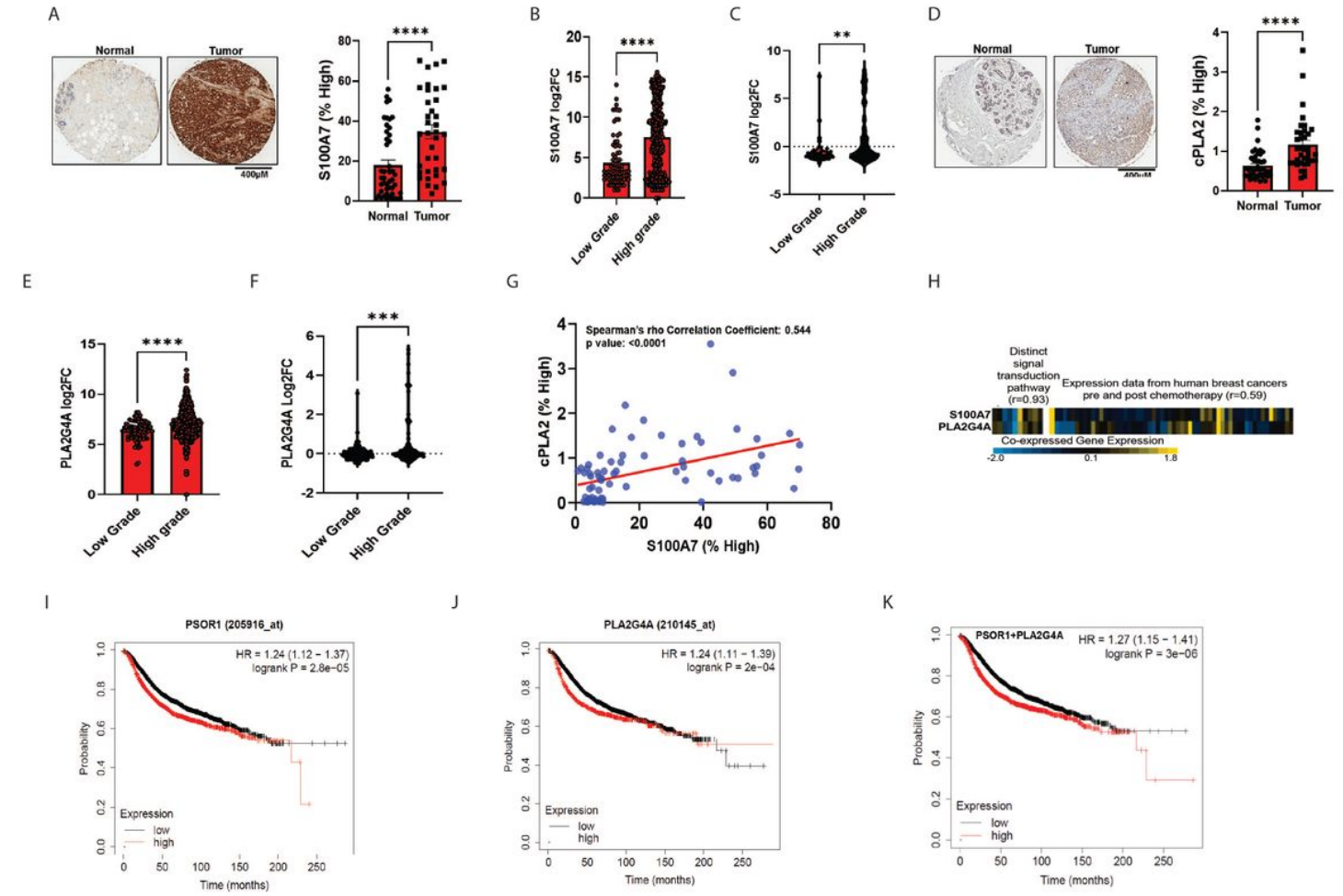

Figure 1

High co-expression of S100A7 and cPLA2 (PLA2G4A) is associated with poor clinical prognosis in breast cancer. Representative immunohistochemistry (IHC) images of (A). S100A7 and (D). cPLA2 proteins in malignant breast tumor samples (n=36) and normal tissues (n=46) [source: US Biomax]. Percent high-positive cells were quantified (right). Non-parametric test (Mann-Whitney U test) was applied. Relative mRNA expression (log2 fold change) of S100A7 and cPLA2 (PLA2G4A) were analyzed in low and high grades of breast tumor tissues using (B & E). GENT2 database (n=532) (http://gent2.appex.kr/gent2/) and (C & F) Caldas (n=113) & Chin, (n=109) datasets. t test was used to calculate the p values. (G). Correlation analysis between S100A7 and cPLA2 protein levels (% high positive) in a tumor tissue microarray (TMAs) of malignant breast cancer patients (n=74). (H). Heatmap showing the correlation of S100A7 and cPLA2 in distinct signal transduction pathways (correlation coefficient = 0.93) and expression in breast tumor tissues of pre-and post-chemotherapy (correlation coefficient = 0.59) (source: Seek database). KM-plotter survival analysis (gene chip) of (I). S100A7 (PSOR1) alone, (J). cPLA2 (PLA2G4A) alone and (K). Combined S100A7 and cPLA2 mRNA expression with recurrence free survival (RFS) (n= 4929) probability of breast cancer patients. ns: non-significant, *P < 0.05, ** P<0.01, *** P<0.001, **** P<0.0001. scale bar: 300μm.

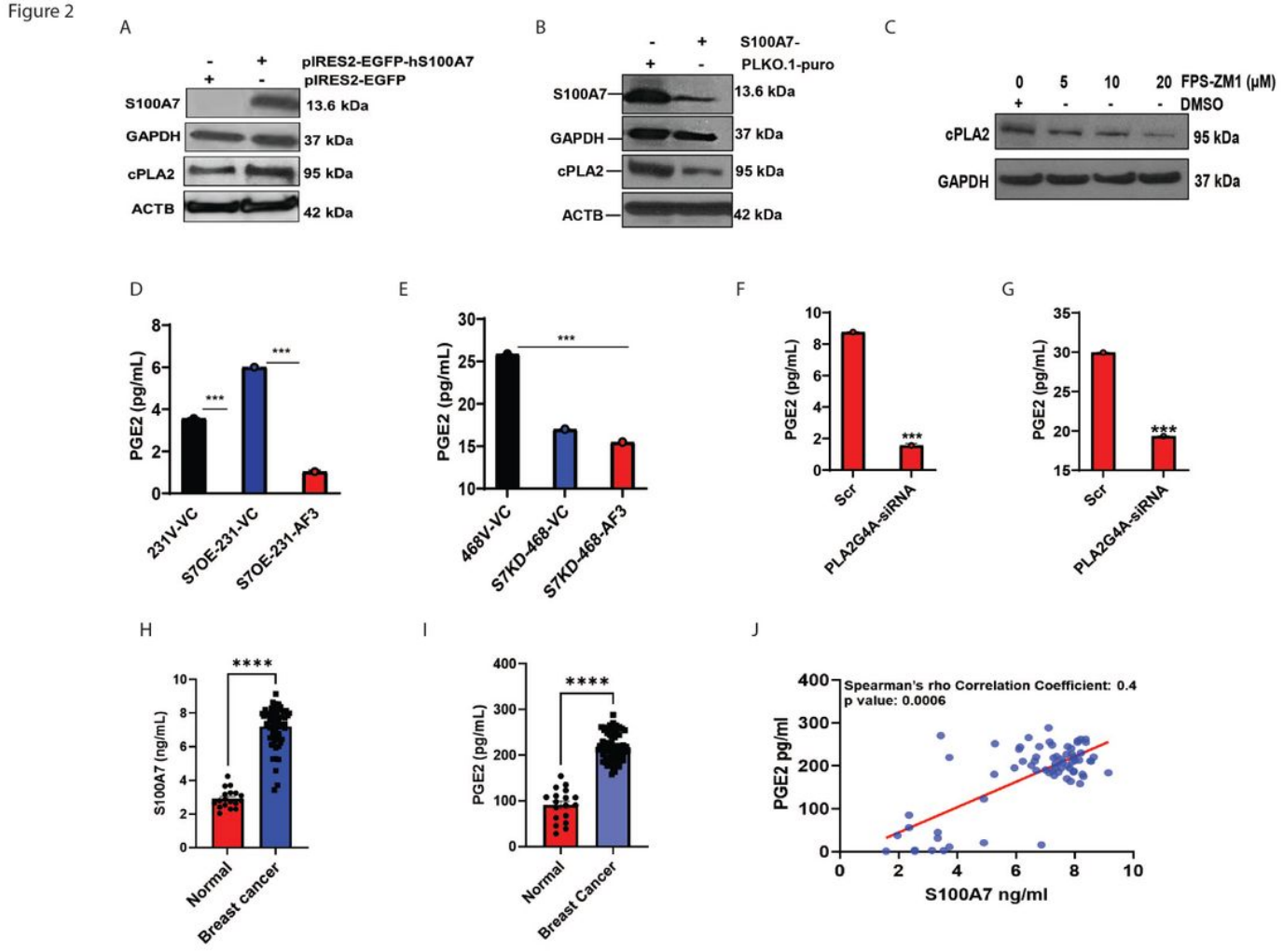

Figure 2

S100A7 regulates cPLA2-mediated PGE2 generation in breast cancer. Immunoblot analysis of S100A7 and cPLA2 proteins in (A). MDA-MB-231 vector (231V) and S100A7 overexpression (S7OE-231) cells. (B). MDA-MB-468 vector (468V) and S100A7 knockdown (S7KD-468) cells. (C). Immunoblot analysis of cPLA2 in S7OE-231 cells treated with vehicle control (DMSO) or RAGE inhibitor (FPS-ZM1) for 24hrs. The bar diagram showing the levels of PGE2 (pg/mL) in conditioned medium (CM) harvested from (D). 231V and S7OE-231 cells, and (E). 468V and S7KD-468 either treated with vehicle control (VC) or AACOCF3 (AF3). Analysis of PGE2 (pg/mL) in CM of (F) S100A7-overexpressing and (G). MDA-MB-468 cells transiently transfected with scramble control (Scr) or PLA2G4A-siRNA. Estimation of (H). S100A7 (ng/mL) and (I). PGE2 (pg/mL) in blood plasma samples of normal subjects (n= 18) and breast cancer patients (n= 62). (J). Correlation between blood plasma level of S100A7 (ng/ml) and PGE2 (pg/ml) in breast cancer patients (n= 70). ns: non-significant, *P < 0.05, ** P<0.01, *** P<0.001, **** P<0.0001. t test and one way ANOVA was used for calculating statistical significance.

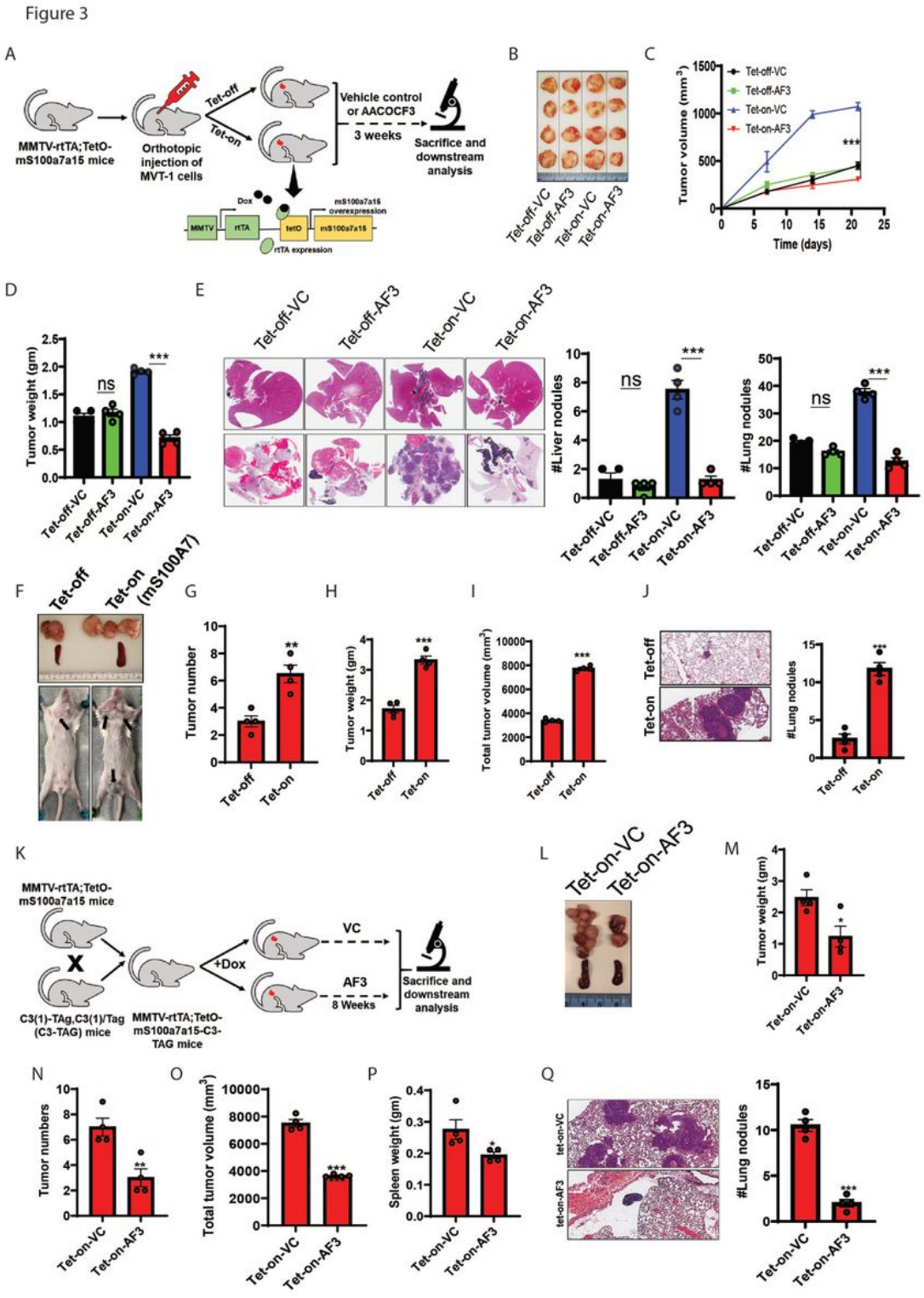

Figure 3

Inhibition of cPLA2 reduces S100A7-enhanced breast tumor growth and metastasis in MMTV-rtTA,TetO-mS100a7a15 bi-transgenic mice model. (A). Schematic representation showing the generation and treatment of the doxycycline (DOX) inducible mS100a7a15 bi-transgenic (Tet-O, tet operator) MVT1 tumor-bearing mouse model. In brief, 1X105 MVT1 cells into the 4th mammary gland (MG) of the bi-transgenic mice. Mice were fed with either 1g/kg.bt. doxycycline diet (Tet-on, n = 8) or normal diet (Tet-off,

n = 8). After the onset of palpable tumors, each group was divided into 2 subgroups (n = 4 each) and were treated with VC or AF3 (5mg/kg.bt) intraperitoneal (i.p.) twice a week for 3 weeks. Tumor volume was measured once a week in these mice. After 21 days, the tumors were harvested from these mice and weighed. (B). Representative photographs of tumors dissected from different experimental groups. (C). Graph showing the tumor volume (mm3) and (D). tumor weight (gm) of each experimental group treated with VC and AF3. (E). Representative image of H&E staining of metastatic nodules in the liver (top) and lung (bottom) of VC and AF3 treated mice. Bar diagram represents the means ±SEMs of four replicates. (F). Representative image showing the tumors harvested from Tet-off (normal diet) and Tet-on (DOX diet) groups with MMTV-rtTA,TetO-mS100a7a15-C3-TAG genotype. Graph showing the (G). the total number of tumors, (H). tumor weight (gm) (I). total tumor volume (mm3) and (J). the number of lung nodules in Tet-off and Tet-on groups. (K). Schematic approach showing the treatment of spontaneous breast cancer model of mS100a7a15 overexpressing (MMTV-rtTA,TetO-mS100a7a15-C3-TAG) mice. MMTV-rtTA,TetO-mS100a7a15-C3-TAG female mice (6 weeks old) were fed with DOX diet (Tet-on) and after the onset of palpable tumors, mice were either treated with VC or AF3 (5mg/kg.bt) intraperitoneal (i.p.) twice in a week for 8 weeks. Tumor volumes were measured externally by using Vernier caliper. At the endpoint, mice were sacrificed and tumors and other organs were harvested for downstream analysis. (L). Photomicrographs of tumors harvested from Tet-on mice treated with VC or AF3. Graph showing the (M). tumor weight (gm), (N). the total number of tumors, (O). total tumor volume (mm3) and (P). Spleen weight (gm) and (Q). the number of lung nodules in Tet-off and Tet-on groups. The graphs indicate the means ±SEMs of four replicates. ns: non-significant, *P < 0.05, ** P<0.01, *** P<0.001. t test and one way ANOVA was used for calculating statistical significance.

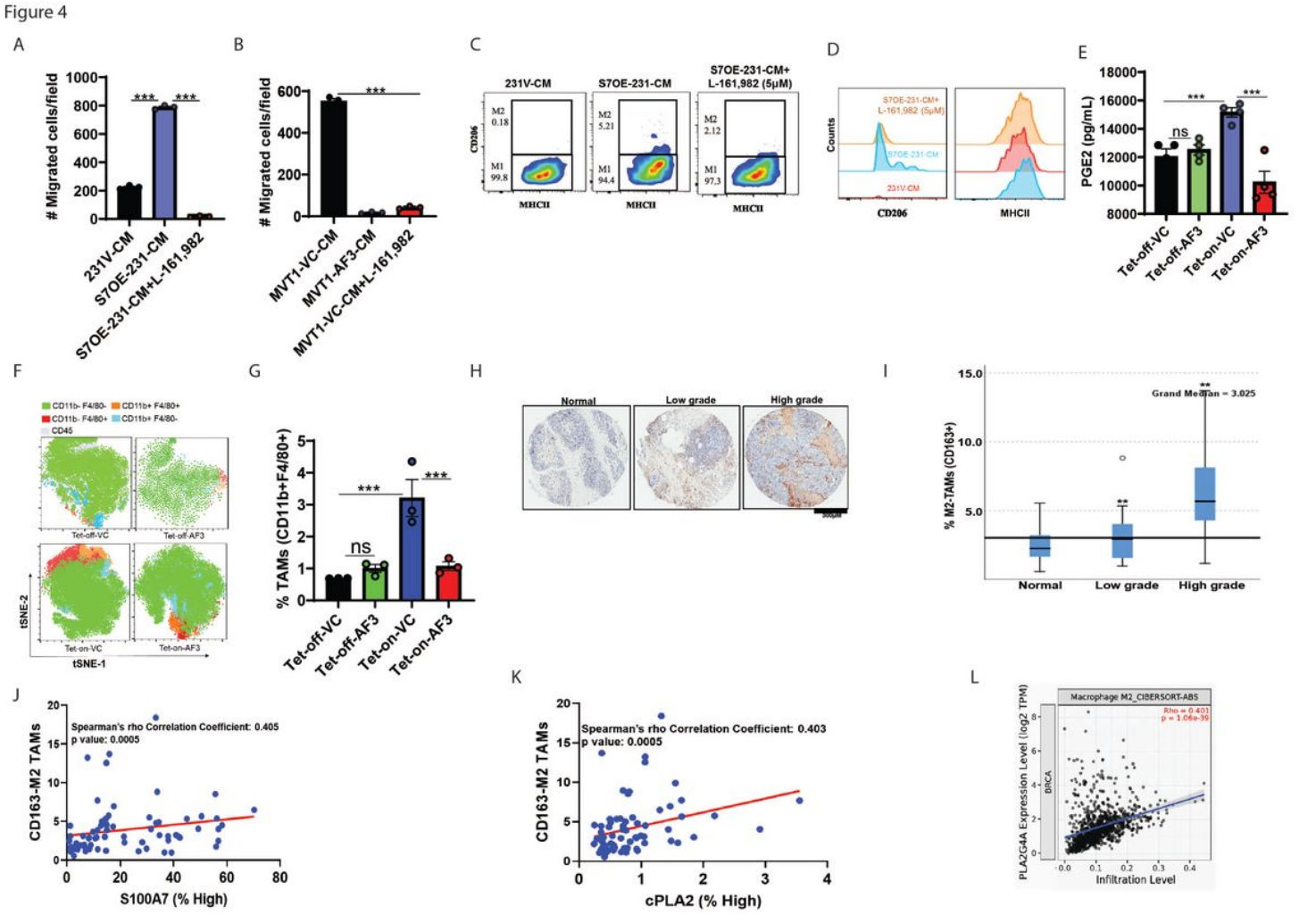

Figure 4

S100A7/cPLA2 signaling enhances the infiltration of tumor-associated macrophages (TAMs) through increased secretion of PGE2. Bar diagram shows the number of migrated bone marrow-derived macrophages (BMDM) per field stimulated with CM derived from (A) 231V and S7OE-231, (B) MVT1 cells treated with VC or AF3 or BMDMs preincubated with EP4 receptor antagonist (5 μM L161,982) for 2hrs before stimulation with CM of MVT1 cells. Overnight migration using transwell inserts was performed. The bars indicate the means ± SEMs of 3 replicates. (C & D). Flow cytometric analysis of MHC-II and CD206 in BMDMs cultured in CM of 231V and S7OE-231 cells or BMDM preincubated with EP4 receptor antagonist (5 μM L161,982) for 2hrs before stimulation with CM of S7OE-231 cells. (E). Quantitative analysis of blood PGE2 (pg/mL) in MVT1 tumor-bearing Tet-off (normal diet) and Tet-on (DOX diet) mice treated with VC or AACOCF3 (AF3). (F). CD11b+F4/80+ TAMs (out of CD45+ cells) in tumors harvested from MVT1 tumor-bearing Tet-off (normal diet) and Tet-on (DOX diet) mice treated with VC or AF3. (G). The bar diagram indicates the means ±SEMs of three replicates. (H). Representative IHC images of CD163+ M2-TAMs in adjacent normal, low-grade, and high-grade invasive breast cancer specimens (source: Biomax). (I). Box plot showing the percentage (%) of CD163+ M2-TAMs in normal, low-grade, and high-grade invasive breast cancer specimens. Non-parametric test (Independent-Samples Median Test)

for comparing high grade to low grade and adjacent normal specimens of breast cancer patients. Bonferroni correction was applied for multiple tests. Spearman rho's correlation coefficient analysis between abundance of CD163+ M2-TAMs with protein levels (% high positive) of (J). S100A7 and (K). cPLA2 in TMAs of breast cancer patients (n=70) (source: Biomax). (L). Spearman rho's correlation coefficient analysis of cPLA2 mRNA (PLA2G4A) expression with infiltration of M2-TAMs in breast cancer patients (source: TIMER2.0, http://timer.cistrome.org/). ns: non-significant, *P < 0.05, ** P<0.01, *** P<0.001. One way ANOVA was used for multiple group comparisons.

Figure 5

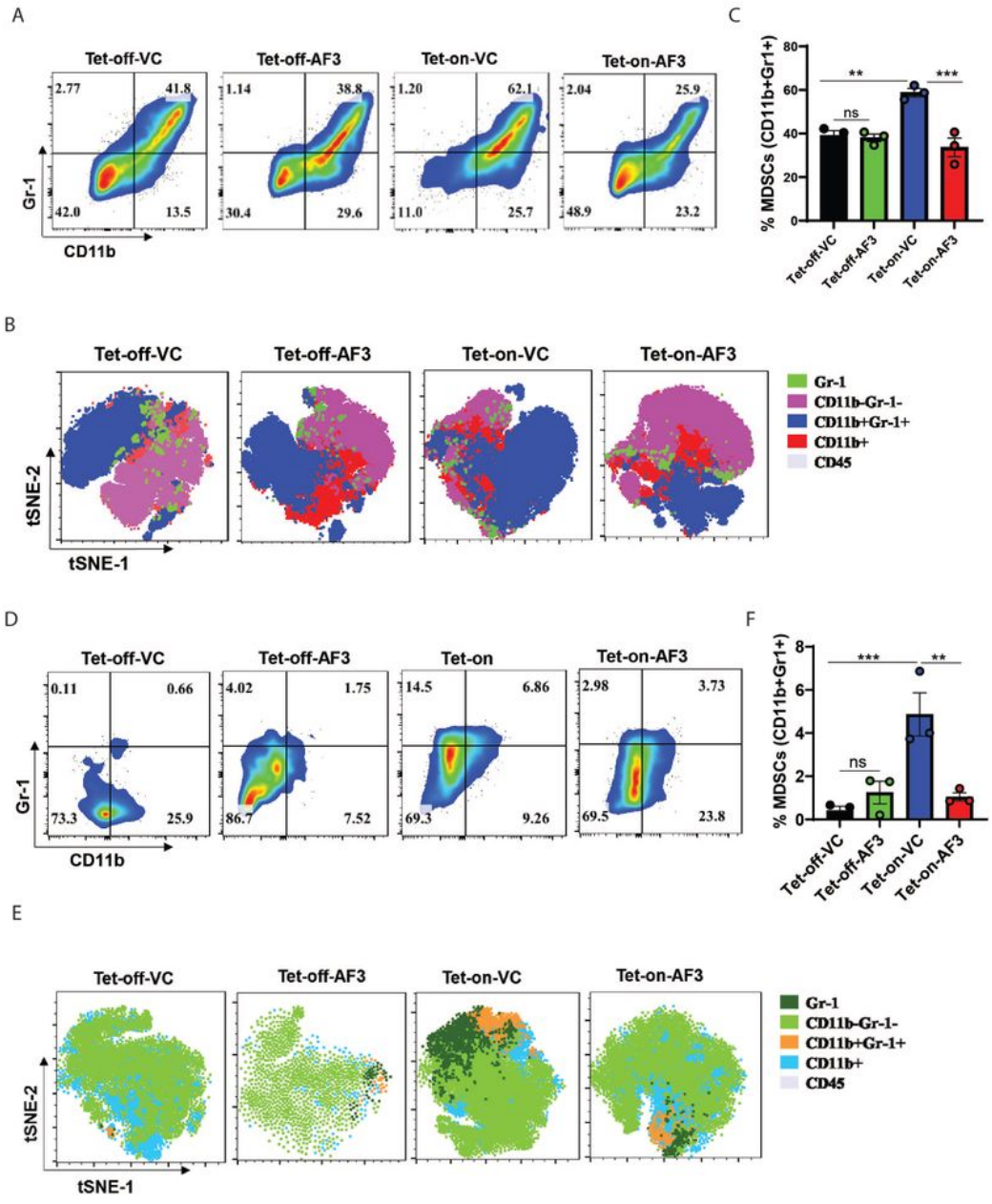

Figure 5

cPLA2 inhibitor decreases S100A7-mediated recruitment of myeloid-derived suppressor cells (MDSCs) in MMTV-rtTA,TetO-mS100a7a15 bi-transgenic mice model. (A). Flow cytometric and (B). t-SNE plot analysis of CD11b+Gr-1+ MDSCs (out of CD45+) in spleens harvested from Tet-off and Tet-on mice treated with VC or AF3. (C). Bar diagram represents the means ±SEMs of three replicates. (D). Flow cytometric and (E). t-SNE plot analysis of MDSCs in tumors harvested from Tet-off and Tet-on mice treated with VC or AF3. (F). Bar diagram represents the means ±SEMs of three replicates. ns: non-significant, *P < 0.05, ** P<0.01, *** P<0.001. One way ANOVA was used for multiple group comparisons.

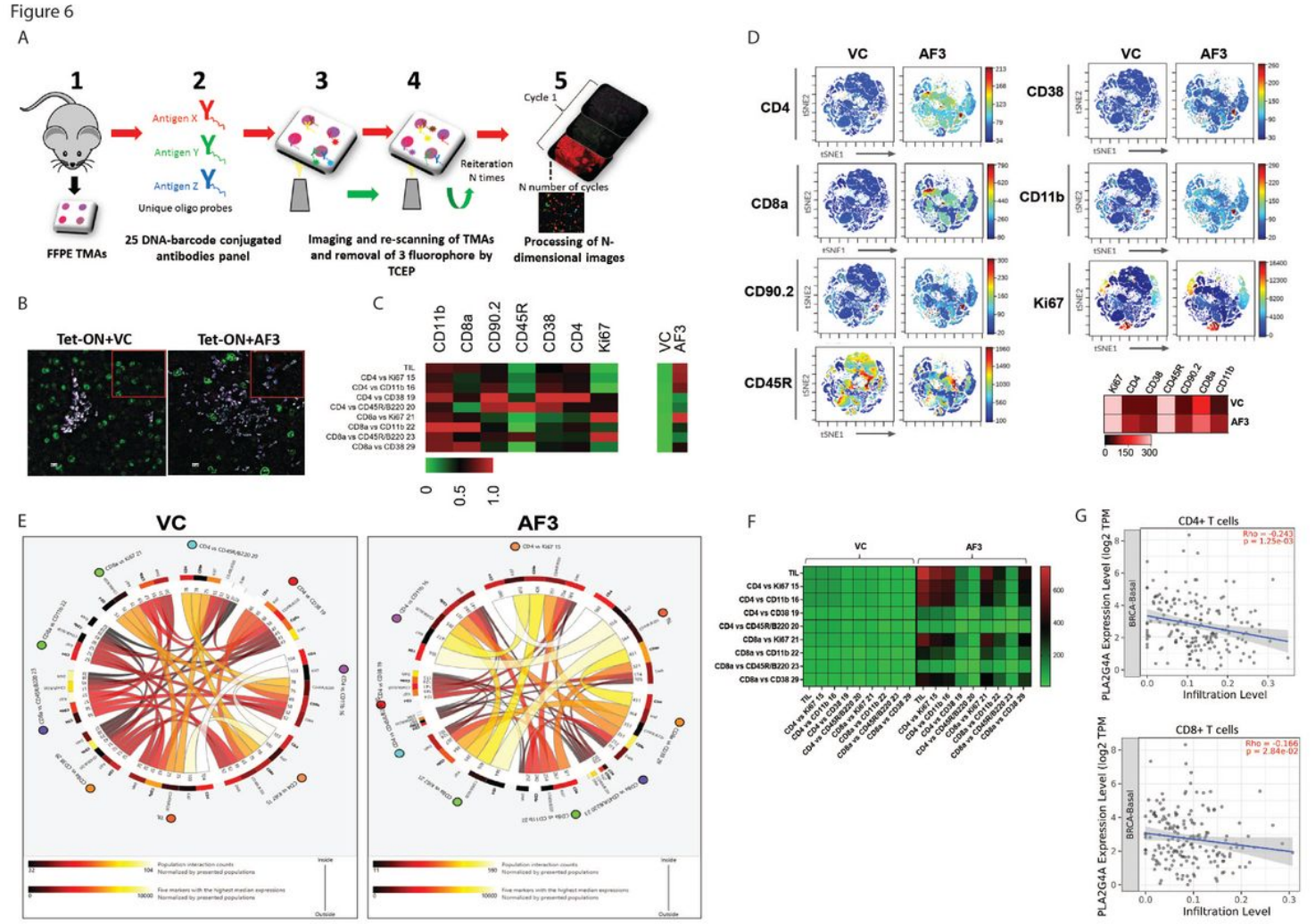

Figure 6

cPLA2 inhibitor increases the infiltration of proliferative activated CD4/CD8 tumor-infiltrating T lymphocytes (TILs) in TME of tumor bearing S100A7 overexpressing mice. (A). Schematic diagram of CODEX workflow showing the different steps of FFPE TMAs staining. (B). Seven-color image of FFPE TMA prepared from of orthotopic syngeneic breast cancer model of mS100a7a15 bi-transgenic mouse model and imaged using a 25 DNA-barcode conjugated antibodies panel. 7 colors show the following markers: red- CD8a, yellow- CD45R, cyan- CD11b, White- CD90.2, blue- CD4, magenta- CD38, and green-

Ki67. (C). Heatmap showing the average strength of cell-type to cell-type interaction for different clusters of vehicle control (VC) and cPLA2 inhibitor (AF3) treated mS100a7a15 overexpression mouse model. (D). t-SNE and heatmap showing the expression of different markers associated with proliferating and activated CD4+ and CD8+ T cells. (E). Circos plot and, (F). heat map showing the cell interaction networks of different subsets of proliferating and activated CD4+ and CD8+ T cells in VC and AF3 treated groups. The thickness of interacting connection associates with the number of contacts, size of the node represents the number of cells per group. Scale bar in heat map showing the interaction strength of different connecting nodes. (G). Spearman rho's correlation coefficient analysis of cPLA2 mRNA (PLA2G4A) expression with infiltration level of CD4 and CD8 T cells in invasive basal-like breast cancer patients (source: TIMER2.0, http://timer.cistrome.org/).

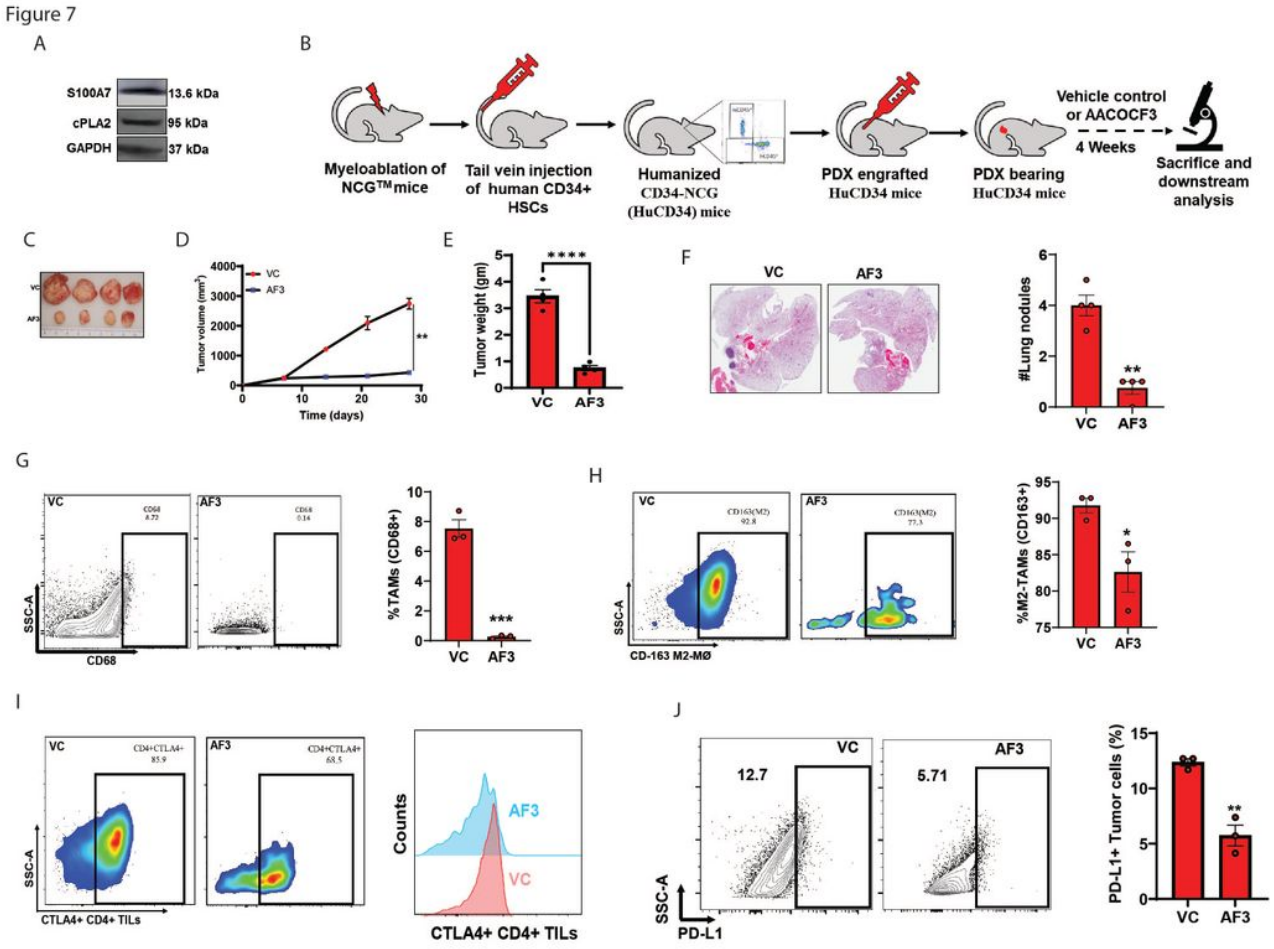

Figure 7

cPLA2 inhibition obstructs tumor growth and metastasis in Hu-PDX mice model by attenuating immunosuppressive cells. (A). Immunoblot analysis of S100A7 and cPLA2 proteins in tumor lysate of breast cancer patient derived-xenograft (PDX) specimen. GAPDH was used as a loading control. (B). Schematic diagram showing the methodology for generation and treatment strategy of humanized PDX (Hu-PDX) breast cancer model. (C). Representative image of tumors harvested from VC or AF3

(5mg/kg.bt) treated Hu-PDX mice model. Graph showing the (D). tumor volume (mm3) and (E). Tumor weight (gm) of VC or AF3 treated PDX mice model. (F). H/E image of lung nodules in lungs harvested from VC or AF3 treated Hu-PDX groups. The graphs indicate the means ±SEMs of four replicates. Flow cytometric analysis of % (G). total CD68+ TAMs (out of EpCAM-), (H). CD163+M2-TAMs (out of EpCAM-CD68+ macrophages) and (I). Exhausted CTLA+ CD4 T (out of EpCAM-CD14-CD3+CD4+) cells (J). PD-L1+ EpCAM+ tumor cells harvested from VC or AF3 treated Hu-PDX groups. The graphs indicate the means ±SEMs of three replicates. ns: non-significant, *P < 0.05, ** P<0.01, *** P<0.001. t test was used for statistical significance.

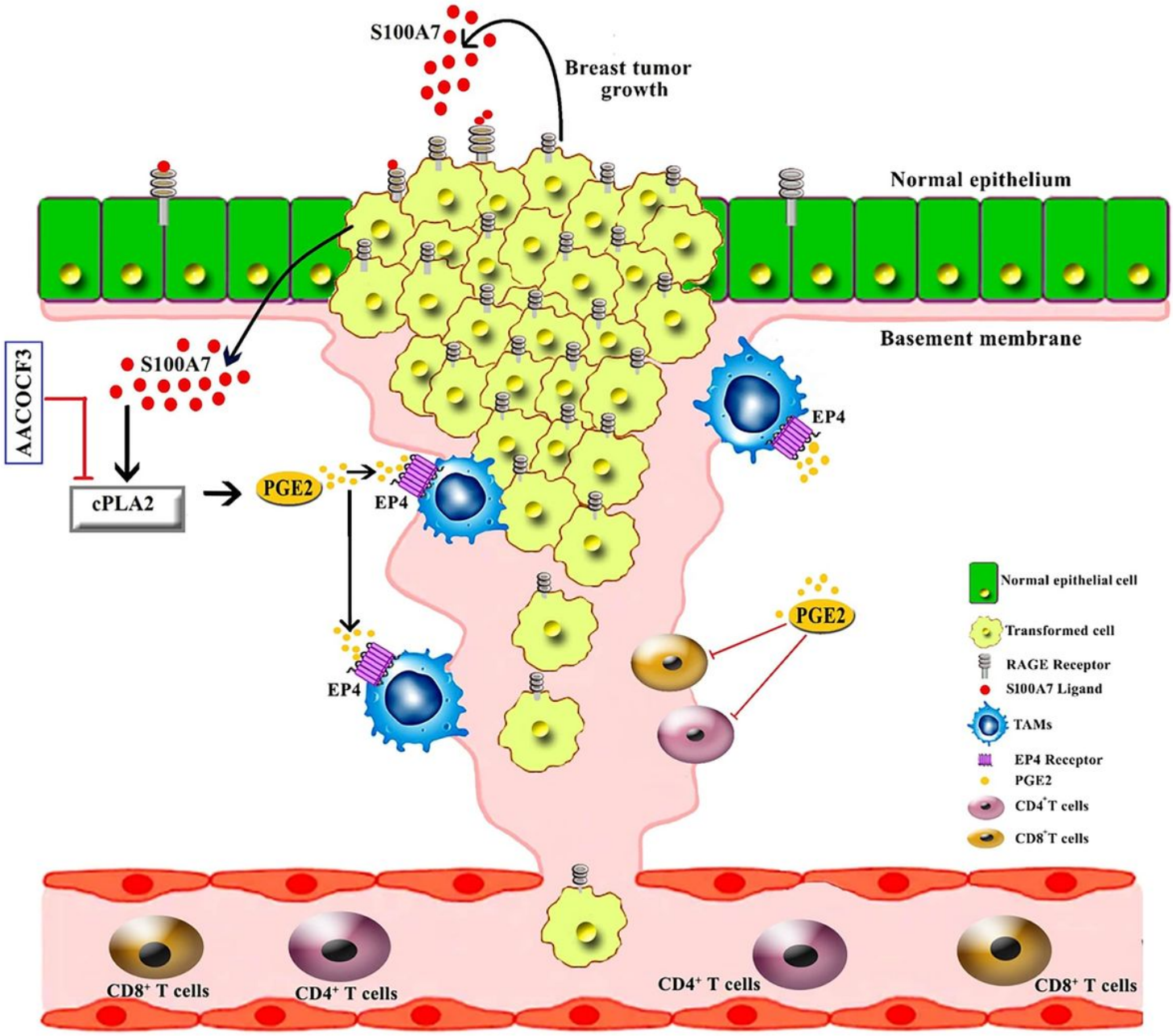

Figure 8

Schematic diagram highlighting S100A7/cPLA2 signaling cascade and its effect on tumor growth and metastasis of invasive breast cancer through modulating the tumor microenvironment (TME).

Supplementary Files

This is a list of supplementary files associated with this preprint. Click to download.

- SupTables.docx
- Supmaterialandmethods.docx
- Suplefiglegend.docx
- Supp.Fig.1.jpg
- Supp.Fig.2.jpg
- Supp.Fig.3.jpg
- Supp.Fig.4.jpg
- Supp.Fig.5.jpg
- Supp.Fig.6.jpg
- Supp.Fig.7.jpg